Spray cone angle prediction model considering nozzle hole geometry

Ibrahim Najar*[1], Benjamin Stengel[1], Fabian Pinkert[2], Bert Buchholz[1], Egon Hassel[3]
[1]Rostock University, Chair of Piston Machines and Internal Combustion Engines, Germany
[2]FVTR GmbH, Rostock, Germany
[3]Rostock University, Chair of Technical Thermodynamics, Germany
*Corresponding author: ibrahim.najar2@uni-rostock.de

Abstract
To understand the influence of the orifice design on the spray spreading angle in conventional direct injection diesel engines, measurements were carried out on a high-pressure high-temperature chamber using three different nozzles and diesel fuel (DIN EN 590). The first nozzle is a cylindrical one, the other two are conical (conicity factor 2.7 and 5.7). Unexpectedly, the nozzle with the highest conicity factor exhibits the largest cone angle. The other two nozzles have nearly a similar value of the angle despite the different geometry.
A CFD-study showed that the turbulent kinetic energy of the conical holes internal flow is smaller than that of the cylindrical one. Furthermore, cavitation occurs within the cylindrical hole, which induces the break-up and enlarges the cone angle. Further investigations were carried out using seven different cone angle models from the literature. The comparison with the experimental values indicated that none of the used models was able to capture the measured trend of the spray dispersion because they do not consider the impact of the modern nozzle geometry parameters (conicity and inlet edge rounding) on the jet spreading angle.
From this background, a new model was developed to determine the spray cone angle of direct injection diesel engines, taking into account the actual nozzle design. The model distinguishes between three different effects of the nozzle geometry on the spray dispersion. Considering a cylindrical orifice with sharp edges, tapering the hole and rounding the inlet edges will lead to a decrease in turbulence intensity and cavitation probability and hence the spray cone angle, and on the other hand, to an increase in the nozzle discharge coefficient and the mean velocity at the orifice exit. The last one induces the aerodynamic interaction between the jet and the surrounding gas and hence the spray dispersion. Therefore, a relationship between the change of spray dispersion and discharge coefficient was assumed. The third effect is caused by the velocity profile relaxation which occurs under the influence of the viscous forces i.e. the velocity gradient after leaving the orifice and its wall boundary conditions. This enhances the break-up in the outer boundary of the jet. Reducing the flow losses causes a steeper velocity gradient in the near wall zone and thus increases the spray dispersion. This increase in the cone angle was assumed to be a function of the orifice conicity factor. The validation of the new model with experiments showed a good agreement with the measurements.

Keywords
Internal combustion engines, Cone angle, Cone angle model, Nozzle hole geometry, diesel spray.

Introduction

Carbon dioxide emitted from diesel engines can be reduced by using alternative fuels with lower carbon fraction or by increasing the engine efficiency which is a difficult challenge for diesel engines manufacturers. Enhancing the diesel engine performance demands improving the engine design, the mixture formation and a careful chose of the combustion concept. The mixture formation in high pressure direct injection engines can be defined as a combination of jet break-up, droplet atomization and heat and mass transfer processes that runs simultaneously. To describe these processes five different micro- and macroscopic parameters are usually used: the Sauter mean diameter, the spray tip penetration, the spray break-up length, the maximum liquid penetration and the spray cone angle. The cone angle can be considered as a measure of the spray growth in the radial direction i.e. a measure of the gas which entrains into the spray. The energy carried by the entrained gas controls the vaporization of spray droplets [22]. In case of high pressure jets, big drops and ligaments detach from the coherent core of the liquid under the influence of turbulence and cavitation induced surface perturbation. The previous described process is called the primary break-up. Beside the influence of cavitation and turbulence, the primary break-up can be affected by relaxation of the velocity profile at nozzle exit as well as by the aerodynamic forces [27]. The last mechanism is very important for the secondary break-up and depends on gas density and injection pressure. Increasing the ambient gas density and the injection pressure leads to enhance the interaction between the spray and the surrounding gas and to increase the spray spreading angle. This effect was observed by several authors e.g. [1], [3] and [11] for gas density and [9] for injection pressure. On the other hand, the orifice geometry, the fuel properties and the pressure boundary conditions play an important role in the other break-up mechanisms (cavitation, turbulence and profile relaxation induced break-up). The dependency of the mixture formation quality on the nozzle

hole geometry has been investigated extensively in the last two decades. The major geometrical parameters are the nozzle hole diameter at the exit (d_o), orifice aspect ratio (L/d_o), number of nozzle holes, hydroerosive rounding of the inlet edges (r) and hole conicity factor (K). K-factor of the nozzle hole can be defined as a tenth of the difference between the inlet and outlet diameter of the orifice hole, where the diameters are in micrometre. Another definition is given by equation 1 which will be used later in this work.

$$K = \frac{d_i - d_o}{L} \cdot 100 \quad (1)$$

Two opinions exist regarding whether the conicity enhance the spreading behavior of the spray or not. Positive conicity factor suppresses the formation of cavitation and the turbulent kinetic energy [28] and can lead to reduce the spray cone angle, see for example [24]. In other works like [23] showed some tapered nozzles larger cone angles than other tapered and cylindrical ones, which indicates, that there is an optimal value of the conicity factor where the cone angle reaches a maximum value (at the same boundary conditions).
To predict the cone angle several 0d-models can be found in the literature, for example [1], [4], [5], [7], [8], [9], and [10]. These models and their ability to capture the spray spreading angle correctly will be discussed in detail later.

Spray angle models

1- Sitkei*:* In his model Sitkei distinguished between turbulent and aerodynamic effects on the spreading of the spray [4]. Using similarity theory he introduced the following equation to predict the cone angle of a spray:

$$\theta = 0.03 \cdot (L/d_o)^{-0.3} \cdot \left(\rho_a/\rho_f\right)^{0.1} \cdot Re^{0.7} \quad (2)$$

In equation 2 L and d_o are the injection hole length and outlet diameter, respectively. ρ_a/ρ_f is the ratio of the air density to the fuel density. Re is the Reynolds number calculated with the nozzle orifice exit using the fuel properties as well as the injection velocity at the nozzle orifice. According to [4] larger nozzle hole diameter (at a nearly constant injection velocity) and higher value of the injection velocity (injection pressure) lead to increase the spray cone angle. The cause of this lies in increasing of Reynolds number and hence the turbulence and the radial components of the fuel velocity.
2- The aerodynamic model: This model is based on an assumption that the atomization of the spray follows the aerodynamic break-up mechanism. In this mechanism, the aerodynamic interaction between the surrounding gas and the injected liquid is responsible for the spray break-up [12]. Theoretical description of this mechanism was introduced by Taylor [13]. He studied the rate of growth of the waves of planer liquid surface induced by the shear between the liquid jet and the ambient gas. Ranz [5] applied Taylor's results with assuming a proportionality relationship between the average dispersion angle and the ratio between the radial and axial droplet velocity. If the radial velocity of the detached droplet is equal to the rate of growth of the wave at the moment of break-up, then the initial angle of the spray can be calculated using the following equation:

$$tan(\theta/2) = \frac{4\pi}{A} \cdot \left(\rho_a/\rho_f\right)^{0.5} \cdot f_m^* \quad (3)$$

A is a proportionality constant which depends on the nozzle design [14]. This constant can be determined from measurement or using an empirical formula (equation 4) suggested by Reitz [6], who confirmed equation 3 experimentally.

$$A = 3 + \frac{(L/d_o)}{3.6} \quad (4)$$

f_m^* is a function of Taylor number i.e. of Taylor viscosity parameter $(\rho_f/\rho_a) \cdot (Re_f/We_f)^2$. For inviscid liquids, this function reaches its maximum value $\sqrt{3}/6$. Equation 3 has been simplified into equation 5 by numerous workers e.g. [15] and [16]. In the simplified equation the function f_m^* becomes equal to its maximum value.

$$tan(\theta/2) = \frac{4\pi}{A} \cdot \left(\rho_a/\rho_f\right)^{0.5} \cdot \frac{\sqrt{3}}{6} \quad (5)$$

3- Hiroyasu and Arai: By assuming a constant spreading angle after the break-up time and using the dimensional analysis of the spray dispersion in [17], the spreading angle of the spray can be expressed as:

$$\theta = 0.05 \cdot \left(\frac{\rho_a \cdot \Delta p \cdot d_o^2}{\mu_a^2}\right)^{0.25} \quad (6)$$

Because the used injection pressure did not cover the condition of high injection pressure, the proportionality constant in equation 6 has been modified (according to [19] in [18]). The modified model is given by:

$$\theta = 0.017 \cdot \left(\frac{\rho_a \cdot \Delta p \cdot d_o^2}{\mu_a^2}\right)^{0.25} \quad (7)$$

Δp is in Pa. In a later publication, Hiroyasu and Arai introduced a new empirical correlation. In [8] they examined the influence of injection pressure on the break-up length as well as on the cone angle. The results showed a dependency between the injection pressure and the spreading angle while the injection velocity lower than 100 m/s, which is needed to form a complete spray, i.e. the velocity corresponded to spray break-up as soon as the fuel is

injected. If the injection velocity is higher than this value, then the dispersion angle becomes independent from injection pressure and can be expressed as:

$$\theta = 83.5 \cdot (L/d_o)^{-0.22} \cdot (d_o/D)^{0.15} \cdot \left(\rho_a/\rho_f\right)^{0.26} \quad 8$$

In contrast to the previous model (equation 6 and 7), the new one takes the nozzle geometry into account by considering of orifice aspect ratio (L/d_o) as well the ratio of the orifice exit diameter and the sac chamber diameter D.

4-Varde: Based on experimental results Varde defined a vector of the variables, which influence the cone angle, equation 9.

$$tan(\theta) = f\left(\, d_o,\, L/d_o\,,\, U_o,\, \mu_f,\, \sigma_f,\, \rho_a,\, \rho_f\right) = B \cdot\ Re_f^{\alpha} \cdot \left(\rho_a/\rho_f\right)^{\beta} \cdot We_f^{\gamma} \quad 9$$

The constant α is equal to $1/3$. Varde extracted this value from [20], where the spray dispersion of low viscosity liquid is experimentally examined. β is estimated as $1/3$ from the best fit to the measured curves. Weber number is used in the last correlation to consider the impact of the atomization on the spreading angle. According to Varde, this art of atomization happens on the spray surface and is induced by the contraction of the jet i.e. depends on the nozzle flow. He suggested the following formula to determine the exponential constant of Weber number:

$$\gamma = \frac{3 - (L/d_o)}{3 \cdot (L/d_o)} \quad 10$$

The experimental results of 10 nozzles with different designs showed a dependency between the proportionality constant B and the nozzle L/d_o-ratio. For diesel application where L/d_o-value usually lower than 6, the constant can be approximated using the following correlation:

$$B = 0.0001 \cdot (L/d_o)^5 \quad 11$$

With further increase of L/d_o-ratio (> 6) the constant is asymptotically equal to 0.7.

5-Naber and Siebers: Another empirical model for the spreading angle was introduced by Naber and Siebers in [1] for non-vaporizing sprays and further developed in [2] for vaporizing conditions. In [1] the impact of various nozzles and injection pressure values as well as different fuels on the spray cone angle was examined. It was observed that the spray dispersion can be captured from equation 12 if the gas density ratios less than 0.1:

$$tan(\theta/2) = C_1 \cdot \left(\rho_a/\rho_f\right)^{0.19} \quad 12$$

The proportionality constant C_1 depends on the orifice geometry parameters other than just the orifice diameter and has a value in the range from 0.26 to 0.4. For density ratios larger than 0.1 the spray tends to behave like gas jets. To consider the influence of vaporization on the cone angle, a second term is introduced in the last formula [2], equation 13.

$$tan(\theta/2) = C_1 \cdot \left[\left(\rho_a/\rho_f\right)^{0.19} - C_2 \cdot \sqrt{\rho_f/\rho_a}\right] \quad 13$$

Whereas C_2 is zero for sprays under non-vaporizing conditions, it has a value of 0.0043 for vaporizing fuel jets.

6-Arrègle et al.: Based on a brief review of the literature, Arrègle et al. defined the following empirical expression of the cone angle [9].

$$tan(\theta/2) \propto\ d_o^{0.508} \cdot \Delta p^{0.00943} \cdot \rho_a^{0.335} \quad 14$$

The constants were obtained from fitting equation 14 to measured spray dispersions for three nozzles with different orifice diameters (but the same orifice length) under various gas densities and injection pressure values.

7-Reddemann: In [10] an optical study has been conducted to analyze the break-up behavior of engine relevant jets. The influence of thirteen different fuels on the spray cone angle was investigated using four dimensionless quantities: Reynolds number Re, Weber number We, Ohnesorge number Oh and the density ratio ρ_a/ρ_f. Note, that the Ohnesorge number is a function of Reynolds and Weber number, so considering just two of these three dimensionless quantities in the model is sufficient. According to the considered dimensionless quantities, six different empirical formulas were introduced. The general form is given by:

$$tan(\theta/2) = C \cdot K_1^m \cdot K_2^n \cdot K_3^o \quad 15$$

In the last equation K_i are the considered non-dimensional numbers, C, m, n and o are model constants. Reddemann suggested to use one of the following equations:

$$tan(\theta/2) = 0.212 \cdot \left(\rho_a/\rho_f\right)^{0.198} \cdot Re^{0.0526} \quad 16$$

$$tan(\theta/2) = 0.293 \cdot \left(\rho_a/\rho_f\right)^{0.225} \cdot Oh^{-0.0558} \quad 17$$

Considering another dimensionless number in these equations did not improve the results.

Experimental setup

Our injection measurements were carried out on a high pressure high temperature chamber with three optical accesses using a common rail injector for medium speed diesel engines, Figure 1. The chamber can be operated

under reactive and inert conditions as well as at temperature and pressure values up to 900 K and 60 bar. For the results presented in this work, the vessel was filled with pressurized air and gave nearly non-vaporizing conditions. The operating points are shown in Table 1. The injector was mounted with a customized flange to achieve a full frame of one injection jet for analysis with a maximum length of 130 mm. The other injection jets were hidden using a deflection cap that was mounted on the injector tip. For quantification of the spray characteristics regarding spray penetration and cone angle image sequences were taken using a Phantom V7.2 high-speed camera. The injection events and the camera were controlled via a main test bench computer. To avoid shot-to-shot deviations average results of at least ten injections were taken.

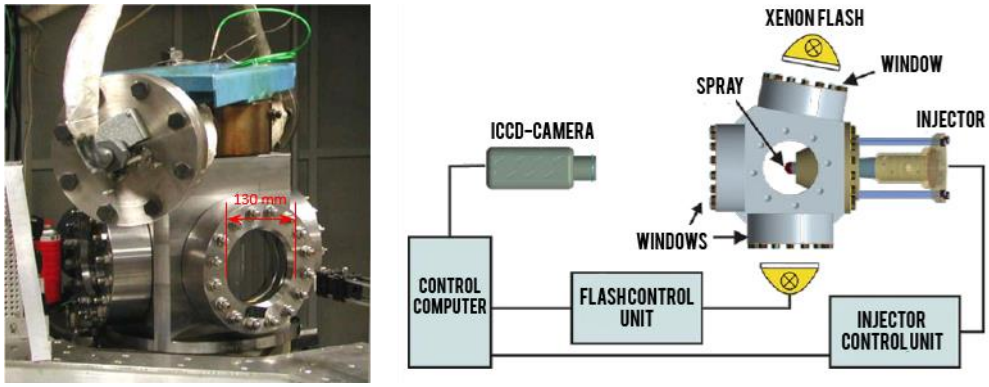

Figure 1. High pressure high temperature chamber (left). Schematic layout of scattered light measurements (right)

Table 1. Test Matrix

Δp in bar	ρ_a in kg/m³	T_a in K
1000	14.25, 28.5 and 42.75	293
1400	14.25, 28.5 and 42.75	293
1600	14.25, 28.5 and 42.75	293

Table 2. Nozzle geometry

Nozzle	K	r in mm	d_i in mm	d_o in mm	C_d
A	0	0.065	0.384	0.384	0.764
B	2.7	0.165	0.388	0.348	0.9267
C	5.7	0.135	0.432	0.346	0.9387

The injector was operated with diesel fuel (DF) according to DIN EN-590 specification using three nozzles with eight injection holes each. To investigate the influence of the orifice wall tapering on the spray cone angle, the conicity factor of these nozzles was increased from zero (cylindrical nozzle) up to 5.7 (high tapered nozzle), see Table 2. The orifice diameter and the edge rounding was changed accordingly to ensure that the nozzles have the same value of the hydraulic flow rate and subsequently to avoid any possible change in the spray spreading angle caused by it. In order to determine the jet cone angle, a MATLAB-program was developed and used to process the captured frames. The spray spreading angle is defined as the angle of an idealized jet (consists of a cone and a half of a sphere) with the same length and projected area as the real spray [3]. More details about the experimental setup can be found in [25] and [26]. The energizing duration of the injector was set to 3 ms for all measured points to assure a long stationary injection process. For result discussion and model validation, values averaged between 2 and 3 ms after Start of Injection SOI are used. The coefficient of variation (CV) of the measured cone angles lies between 5 and 8% for all nozzles.

Experimental Results and discussion

The left diagram in Figure 2 shows the cone angle values for nozzle A at all injection pressures and gas densities. As expected and observed by numerous workers, increasing the gas density leads to higher values of the jet spreading angle. It can be noticed that the jet spreads wider if the injection pressure is increased. The reason for this lies either in the high values of the Reynolds number of the internal nozzle flow and/or in the intensive interaction between the injected fuel and the surrounding gas. In the present work, just one fuel was used and hence the influence of Reynolds number on the jet spreading angle could not be investigated. However, increasing the injection pressure from 1000 bar up to 1600 bar leads to an absolute and relative increase in the spray dispersion smaller than 0.75° and 5%, respectively.

The right diagram in Figure 2 presents a comparison between the measured cone angles of the three used nozzles. From this diagram, it can be observed that nozzle A and B exhibit similar values of the cone angle, especially at

high gas densities. Furthermore the nozzle with the highest conicity factor shows the largest cone angle as can be noticed from the same diagram. Interesting is that the tapered nozzles (B and C) have nearly the same orifice exit diameter (see Table 2) and in this case the same mean velocity and discharge coefficient because the hydraulic flow rate of the nozzles has the same value. This confirms that tapering the orifice walls and rounding the inlet edges affect the cone angle in some way.

For further investigation, the nozzle internal flow was numerically calculated using the commercial code AVL-Fire. The transient multi-phase CFD-simulation showed that the cavitation occurs just in nozzle A (the cylindrical nozzle). In addition, and because of flow separation from the nozzle wall at orifice inlet, the internal flow of the cylindrical nozzle has the highest value of the turbulent kinetic energy. Both phenomena (cavitation and turbulence) induce the spray primary break-up and enhance the spreading behavior of the jet. According to the previous discussion, a higher value of the spray spreading angle is expected from nozzle A, which is not the case.

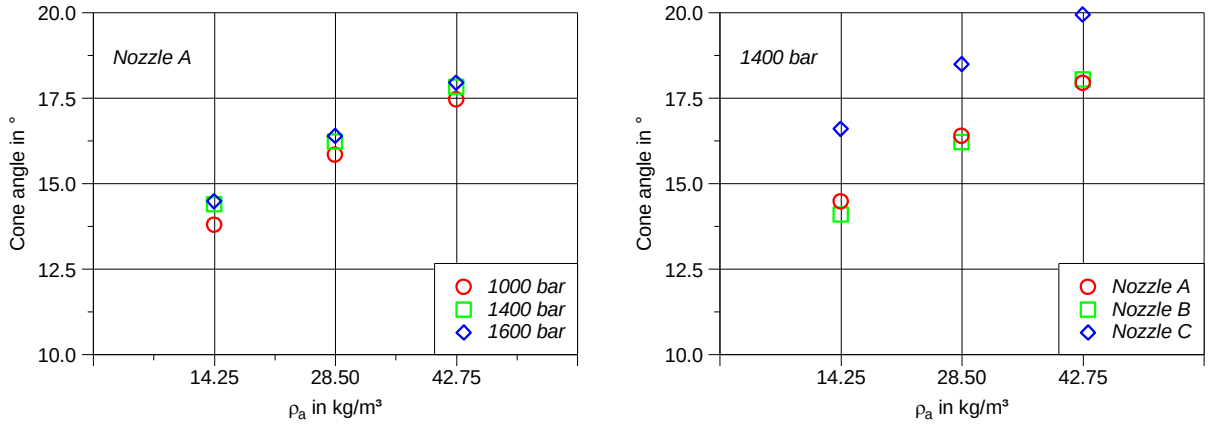

Figure 2. Spray spreading angle of Nozzle A at all boundary conditions (left) and of all nozzles at various gas densities and 1400 bar injection pressure (right)

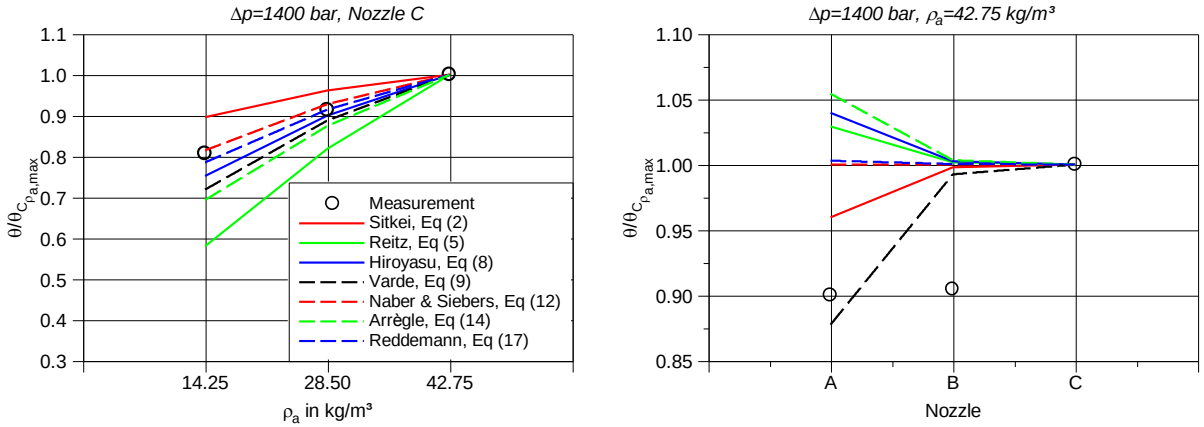

Figure 3. Normalized cone angles for nozzle C at all analyzed gas densities (left) and for the maximum gas density and all nozzles (right)

Validation of the models from literature

Figure 3 presents a comparison between the measured and calculated cone angles using the above-described models. To avoid any possible deviation caused by the definition of the spreading angle and the jet boundary as well as by the experimental settings the results from each model are normalized using the cone angle value of nozzle C from the same model at the highest injection pressure and gas density. The diagram on the left-hand side of Figure 3 reveals the normalized calculated and measured cone angles for nozzle C at various gas densities. From this plot, it can be observed that all models show the exponential dependency of the jet spreading angle on the gas density. The differences between the models lie in the magnitude of the dependency i.e. in the exponential constant value. It can also be observed that equation 12 and 17 (Naber & Siebers and Reddemann) exhibit the best fit to the experimental results. The right diagram of Figure 3 can be used to make a statement regarding the effect of nozzle hole geometry on the jet spreading behavior. Just equation 2 and 9 capture the trend correctly because they overestimated the influence of the orifice aspect ratio L/d_o. This can be observed by comparing the measurements with the equations for nozzle A and B. From the same diagram can be noticed that all models estimate nearly the same value for nozzle B and C because these nozzles have the same exit diameter and aspect ratio.

Model development and validation

To develop the new model two basic assumptions have been made:

1- A relationship is assumed between the cone angle in the zone far from the nozzle tip, where the mixture behaves like a two-phase flow, and the initial angle resulted from the primary break-up of the liquid jet.

2- An initial geometry is assumed for each orifice, before rounding the edges and tapering the walls. Then the discharge coefficient of the real hole can be expressed as:

$$C_d = C_{di} + \Delta C_d \qquad 18$$

In the last equation C_{di} and ΔC_d represent the discharge coefficient of the initial hole and the change of the discharge coefficient caused by the geometry, respectively. The initial hole is assumed to be a cylindrical one with sharp edges and *a diameter equal to the inlet diameter of the real orifice*. C_{di} can be estimated using equation 19 which results from a numerical study of the internal nozzle flow of eleven different initial holes (from 150 up to 400 µm with 25 µm steps in between).

$$C_{di} = 0.654 \cdot d_i^{0.007} \qquad 19$$

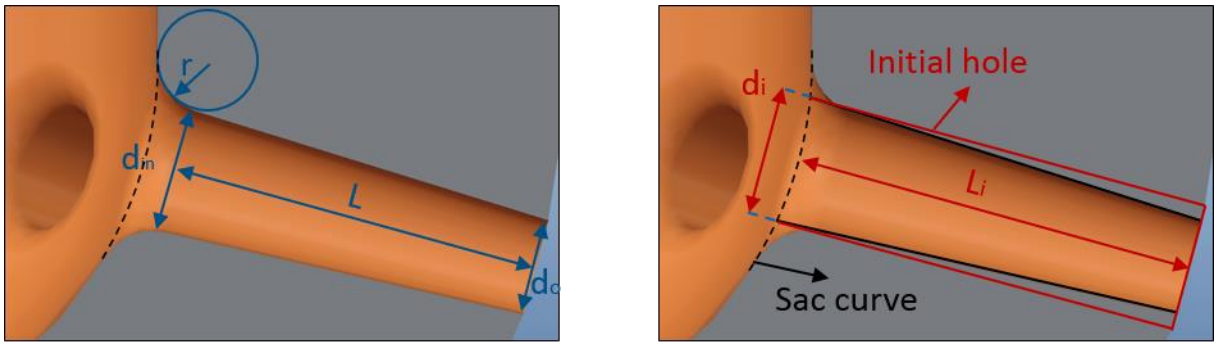

Figure 4. The real geometry (left) and the initial hole (right)

The first step in the model development is to distinguish between the effect of the boundary conditions (injection pressure and gas density) and the geometrical parameter on the cone angle. Accordingly, the spray dispersion of the initial hole can be mathematically expressed as:

$$\theta_i = \alpha \cdot \left(\rho_a/\rho_f\right)^{\beta} \cdot \Delta p^{\gamma} \cdot d_i^{\delta} \qquad 20$$

α and β are the proportionality constant and the exponential factor of the gas density (or here the ratio of the gas and fuel density), respectively. γ takes into account the influence of the injection pressure on the spray dispersion. δ accounts for the dependency of the jet dispersion angle on the initial hole diameter (which is the diameter at the real hole entrance). The previous equation should be modified for real orifices with real geometry, equation 21.

$$\theta = \theta_i \cdot G = \alpha \cdot \left(\rho_a/\rho_f\right)^{\beta} \cdot \Delta p^{\gamma} \cdot d_i^{\delta} \cdot G \qquad 21$$

The parameter G considers the influence of the nozzle hole geometry on the cone angle. Based on the first assumption, the dependency of the jet dispersion on the orifice shape can be analysed via the influence of orifice geometry on the primary break-up process, which is simplified as follows:

1- Positive conicity factors and higher value of the orifice inlet radius lead to increase in the hydraulic flow rate and to suppress the formation of cavitation and reduce the turbulence intensity and hence the jet spreading angle. This effect is assumed to be an exponential function of the ratio between the change in the discharge coefficient ΔC_d and the discharge coefficient itself i.e.between the initial discharge coefficient C_{di} the real one C_d, equation 22.

$$G_1 = (C_{di}/C_d)^{\varepsilon} \qquad 22$$

2- Tapering the hole and rounding the edges lead to reduce the hydraulic losses and to enhance the discharge coefficient and as a result of this to increase the mean velocity at nozzle exit, the aerodynamic forces acting on the spray and hence the cone angle. This effect is similar to the influence of the injection pressure on the jet dispersion. From comparing the hydraulic flow rate of the initial and real orifice the following correlation results to predict the influence of the previous effect on the cone angle:

$$G_2 = (C_{di}/C_d)^{-2\gamma} \qquad 23$$

3- The interaction between the flow and the tapered walls leads to a higher gradient of the velocity in the flow layers near the wall i.e. the hydraulic force acting on the wall. After leaving the orifice and its wall boundary conditions, the velocity profile relaxation occurs under the influence of the viscous forces i.e. the velocity gradient. This enhances the break-up in the outer boundary of the jet and therefore the spray dispersion behavior. To consider the profile relaxation caused by the velocity gradient the following formula is suggested:

$$G_3 = 1 + 0.05 \cdot K \qquad 24$$

Substituting equations 22, 23 and 24 into equation 20, the following equation is obtained:

$$\theta = \alpha \cdot \left(\rho_a/\rho_f\right)^{\beta} \cdot \Delta p^{\gamma} \cdot d_i^{\delta} \cdot G_1 \cdot G_2 \cdot G_3 = 10.5 \cdot \left(\rho_a/\rho_f\right)^{0.22} \cdot \Delta p^{0.11} \cdot d_i^{-0.5} \cdot \left(C_{di}/C_d\right)^{0.53} \cdot (1 + 0.05 \cdot K) \qquad 25$$

Figure 5 shows the validation of the last correlation for all nozzles. As can be noticed, the calculated values of the spreading angle agree very well with the experimental data. The maximum absolute and relative deviations are 1 degree and 6%, respectively. This deviation occurs at nozzle C at the highest injection pressure and the smallest gas density. Diagram *d* in the same figure summarizes the results for 1400 bar and 42.75 kg/m³ by presenting the spreading angles of the three nozzles normalized by the angle value of nozzle C at the same boundary conditions. The diagram confirms the ability of the new model to capture the influence of the orifice shape on the jet cone angle.

Table 3. Constant values used for equation 25

α	β	γ	δ	ε
10.5	0.22	0.11	-0.5	0.75

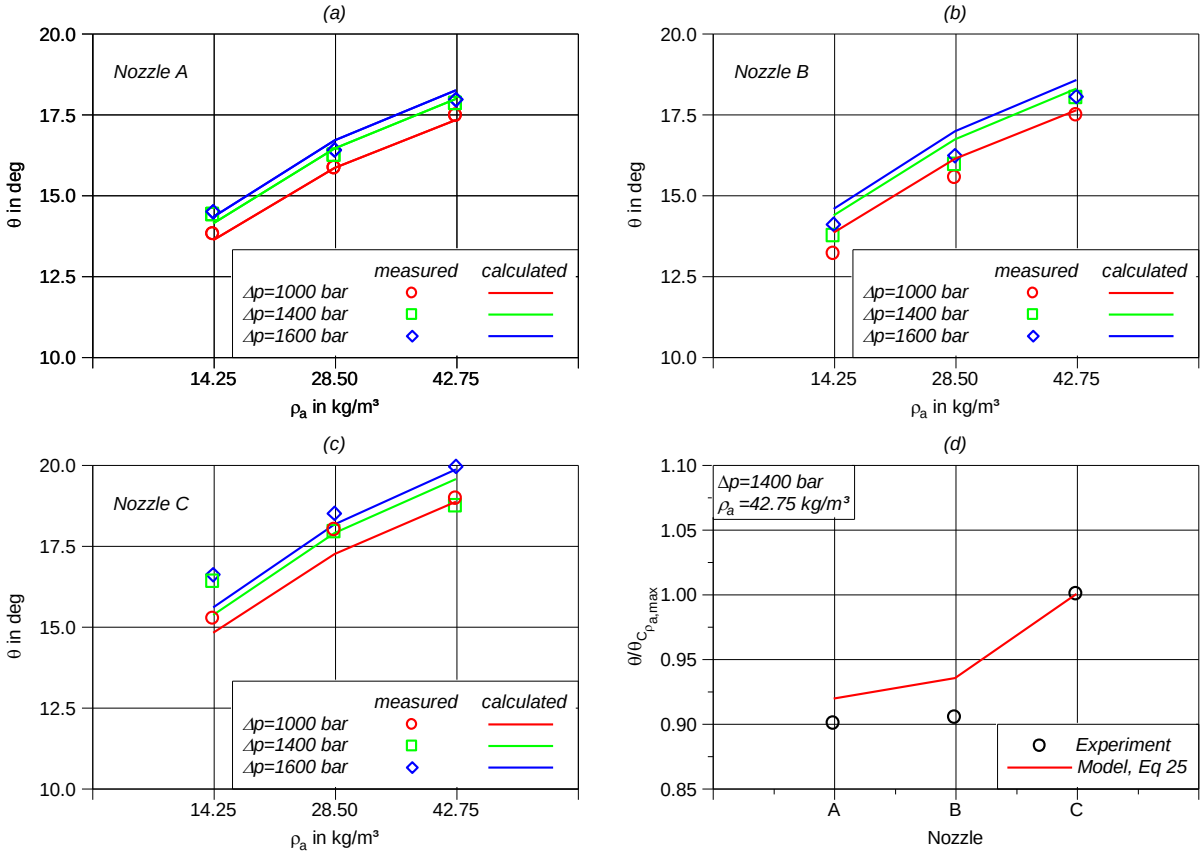

Figure 5. Measured and calculated spreading angles for the three nozzles at all boundary conditions (diagram *a, b* and *c*) and the normalized angles at 1400 bar and 42.75 kg/m³ (*d*)

Conclusions

One of the key parameters which control fuel evaporation, combustion and emissions in conventional direct injection diesel engines is the spray cone angle. To investigate the influence of the nozzle geometry on this parameter, measurements were carried out on a high-pressure high-temperature chamber using three nozzles with different orifice shape and diesel fuel (DIN EN 590). The experimental study confirmed, that the nozzle geometry (conicity factor and rounding of the inlet edges) affects the spreading angle significantly. Contrary to the initial expectations, the nozzle with the most tapering walls (nozzle C) exhibited the largest value of the cone angle at all examined conditions. Despite the cavitation and the high turbulence intensity the cylindrical nozzle (nozzle A) shows a dispersion behavior similar to nozzle B (with K-factor of 2.7).

For further investigations calculated values using seven different cone angle models from the literature were compared to the experimental results. The comparison indicated that none of the used models is able to predict the measured trends of the spray dispersion correctly because these consider the nozzle geometry via simple functions of the outlet diameter and/or the orifice aspect ratio. From this background, a new model was developed to predict the spray cone angle with considering the actual nozzle design. For this reason it was assumed that the measured cone angle is related to the initial angle resulted from the jet primary break-up. Therefore, the nozzle geometry

influence on the cone angle can be analyzed by discussing how this geometry affects the primary break-up. It can be distinguished between three different effects of the geometry on the cone angle. Tapering the wall edges and rounding the inlet edges leads to suppress the cavitation formation and decreases the turbulence intensity and hence the jet spreading angle. On the other hand, these proceedings reduce the flow hydraulic losses and increase the mean velocity at the hole exit and enhance the dispersion of the spray similarly to the injection pressure. These two effects were taken into account as functions of the relative change in the discharge coefficient. To estimate this change a new orifice was introduced as the injection hole in the initial situation. This initial hole is a cylindrical hole with sharp edges. The initial diameter is the inlet diameter of the real orifice. From a numerical study, a new equation was developed to predict the discharge coefficient of this initial hole.
A further effect of the nozzle geometry on the cone angle is caused by the profile relaxation which occurs under the influence of the viscous forces i.e. the velocity gradient, especially in the outer spray zone. The last effect was assumed to be a function of the conicity factor.
Combining these three effects with considering the dependency of the cone angle on the gas density, injection pressure, and inlet diameter leds to a new correlation to predict the jet spreading angle. This model is validated using experimental results and is very well able to capture the relationship between the cone angle and the nozzle geometry correctly.

Acknowledgements
The presented results are part of the research project “Multiple Injection Strategies for Optimizing Mixture Formation and Combustion in Large Diesel Engines to meet the lowest CO_2 and Pollutant Emissions using Maritime Fuels”, Project number 286815162. We would like to thank the German Research Foundation (DFG) for funding this project.

Nomenclature

K	conicity factor	ρ	density [kg/m³]	σ	surface tension [N/m]
L	orifice length [mm]	T	temperature [K]	μ	viscosity [Pa.s]
d	orifice diameter [mm]	θ	cone angle [°]	Re	Reynolds number
D	sac diameter [mm]	U	mean velocity [m/s]	We	Weber number
r	inlet edge radius [mm]	Δp	injection pressure [bar]	Oh	Ohnesorge number
f_m^*	Taylor function	*SOI*	Start of Injection	*CV*	Coefficient of Variation

Subscripts

i	orifice inlet, initial hole	*a*	ambient gas
o	orifice outlet	*f*	fuel

References

[1] Naber, J. and Siebers, D., SAE Technical Paper 960034, https://doi.org/10.4271/960034.
[2] Siebers, D., SAE Technical Paper 1999-01-0528, 1999, https://doi.org/10.4271/1999-01-0528.
[3] Fink, C., Ph.D. thesis, University of Rostock, Germany, 2011
[4] Sitkei, G., Springer Verlag, 1964, ISBN 978-3-662-12199-3
[5] Ranz, W. E., The Canadian Journal of Chemical Engineering 36.4 (1958): 175-181.
[6] Reitz, R. and Bracco, F., SAE Technical Paper 790494, 1979, https://doi.org/10.4271/790494.
[7] Varde, K. S., The Canadian journal of chemical engineering 63.2 (1985): 183-187.
[8] Hiroyasu, H. and Arai, M., SAE Technical Paper 900475, 1990, https://doi.org/10.4271/900475.
[9] Arrègle, J., et al., SAE Technical Paper 1999-01-0200, 1999, https://doi.org/10.4271/1999-01-0200.
[10] Reddemann, M. A., Ph.D. thesis, RWTH Aachen University, Aachen, Germany, 2015.
[11] Najar, I., Ph.D. thesis, University of Rostock, Germany, 2016
[12] Castleman, R. A., US Department of Commerce, Bureau of Standards, 1931.
[13] Taylor, G. I., Reprinted in The Scientific Papers of Sir Geoffrey Ingram Taylor, Vol. 3." (1963): 244-255.
[14] Reitz, R. D., and Bracco. F. V. The physics of Fluids 25.10 (1982): 1730-1742.
[15] Chehroudi, B., et al., YSAE Technical Paper 850126, 1985, https://doi.org/10.4271/850126.
[16] Heywood, J. B. "Internal combustion engine fundamentals," McGraw-Hill, Inc. 1982
[17] Wakuri, Y., Fujii, M., Amitani, T., and Tsuneya, R., Bull JSME 1960; 3(9):123–30.
[18] Arai, M., International Conference on Liquid Atomization and Spray Systems, Heidelberg, Germany, 2012
[19] Zama, Y., Ochiai, W., Furuhata, T., and Arai, M., Proceedings of ILASS-Asia 2011, Taiwan, Oct., 2011.
[20] DeJuhasz, K. J., Zahn, O. F., and Schweitzer, P. H., (No. 40). The Pennsylvania. 1932
[21] Schneider B., Ph.D. thesis, No. 15004, ETH Zurich, 2003.
[22] Siebers, D., SAE Technical Paper 980809, 1998, https://doi.org/10.4271/980809.
[23] Gostić, I., Ph.D. thesis, ESYTEC, Energie-und-Systemtechnik-GmbH, 2011, Germany
[24] Yu, S., Yin, B., et al. International Conference on Liquid Atomization and Spray Systems, USA, 2018
[25] Buchholz, B., Ph.D. thesis, University of Rostock, Germany, 2008
[26] Pinkert, F., Ph.D. thesis, University of Rostock, Germany, 2016
[27] Baumgarten, C., Springer Science & Business Media. ISBN 978-3-540-30835-5
[28] Soriano Palao, O., et al., SAE Technical Paper 2011-28-0120, https://doi.org/10.4271/2011-28-0120.